Title: Changing ice seasons and phenology affects under-ice lake thermal dynamics

Running head: Changing under-ice thermodynamics

Author names: Isabella A. Oleksy*[a], David C. Richardson[b]

Affiliations:

[a] Department of Zoology and Physiology, University of Wyoming, Laramie, USA

[b] Biology Department, SUNY New Paltz, New Paltz, NY, USA

*Corresponding author

Abstract:

Temperate lakes worldwide are losing ice cover, however implications for under-ice thermal dynamics are poorly constrained. Using a 90-year record of ice phenology from a temperate lake, we examined trends, variability, and drivers of ice phenology. The onset of ice formation decreased by 2.3 days decade^{-1} which can be largely attributed to warming air temperatures. Ice-off date has become substantially more variable with spring air temperatures and cumulative February through April snowfall explaining over 80% of the variation in timing. As a result of changing ice phenology, total ice duration consequently contracted by a month and more than doubled in variability. Using weekly under-ice temperature profiles for the most recent 36 years, shorter ice duration decreased winter inverse stratification and extended the spring mixing period. These results illustrate how changing ice phenology can affect summer thermal dynamics.

Scientific Significance Statement:

Lakes worldwide are losing ice cover in response to climate change. We used a rare and nearly century-long dataset of ice formation and ice clearance records to examine trends, variability, and their drivers. We found that ice cover is getting substantially shorter and more variable with winter ice duration about a month shorter now than it was a century ago. Using under-ice temperature measurements from the most recent three decades, we find differences in under-ice temperatures affected by lake ice duration. We expect shorter ice seasons with high year-to-year variability and more frequent years of intermittent ice cover, shifting the mixing dynamics of many temperate lakes from twice to once per year.

Keywords: phenology; lake ice; variability; climate change; long-term trends; trend analysis

Data availability statement:

All ice phenology data are published in Sharma et al., 2022. Under-ice temperature profile data are published in Mohonk Preserve et al., 2020. Daily air temperature and precipitation data from the Mohonk Preserve Weather station are available from the US Weather Bureau/National Weather Service rain gauge (Network ID GHCND:USC00305426).

Introduction

Ice cover is one of the longest measured indicators of climate change in lake ecosystems (Magnuson et al., 2000; Robertson et al., 1992). The role of under-ice ecology is increasingly recognized as an integral control of open-water lake ecosystem dynamics (Hampton et al., 2017; Salonen et al., 2009). However, widespread changes in lake ice phenology are occurring around the world and many once permanently ice-covered lakes have transitioned toward intermittent cover because of global anthropogenic climate change and teleconnections, which exert control on regional and local weather conditions and thus lake ice phenology (Sharma et al., 2019). Lake ice, and the timing of its formation and clearance, affects many lake ecosystem properties such as oxygen dynamics, timing of stratification, and lake productivity (Jansen et al., 2021).

Two distinct phases of lake thermal dynamics under ice have been currently identified and are dependent on lake morphometry and local climatic conditions (Kirillin et al., 2012). The first phase is characterized by release of heat from the sediments that has accumulated in the ice-free season. The second phase is typically characterized by inverse stratification; however, the duration of inverse stratification appears to be decreasing in lakes globally (Woolway et al., 2022). Predicting how ongoing changes in lake ice phenology will alter annual, whole-lake ecosystem function first requires an understanding of the drivers of trends and variability around those trends (Wilkinson et al., 2020). While lake ice phenology records are common, observations of multi-decadal under-ice thermal properties are comparatively rare (e.g., Sharma et al., 2022). Under-ice temperatures are critical in contextualizing the physical, chemical, and biological implications of increasingly shorter and potentially variable ice phenology.

We analyzed a 90-year record of both ice-on and ice-off observations from a small, mountain lake in New York, USA (Sharma et al. 2022). We combine the long-term ice phenology record with weekly under-ice thermal profiles from the most recent 36 years to ask the following questions. First, is ice phenology and variability changing? Second, what local meteorological and global scale climatic

variables explain variability in lake ice phenology? Third, how does ice phenology affect underwater winter stratification, temperature, and mixing dynamics?

Methods

Site description and data collection

Mohonk Lake (41.766°N, -74.158°W) is a deep (18.5 m maximum depth), small (6.9 ha), dimictic, oligo-mesotrophic mountain lake located on the Shawangunk Ridge, New York State, USA (Oleksy and Richardson 2021; Richardson et al. 2018). The lake's surface area occupies 40% of the watershed in a small glacier-formed depression on the Shawangunk Ridge (Richardson et al., 2018). Ice-on day was recorded as the first day with 100% ice coverage; ice-off day was recorded as the first day with 0% ice cover from 1932-2022 (Sharma et al. 2022). Ice phenology was recorded in a consistent manner over the entire 90-year data record with only seven years missing ice-on data (all earlier than the 1954 water year) and one year of missing ice-off record in the 1965 water year (Sharma et al. 2022). Over the entire ice record, maximum, minimum, and average daily air temperature (°C) and snow and precipitation (mm) were measured within 50 m of the lake at a National Weather Service station (Network ID: GHCND:USC00305426). From 1985-2022, profiles of lake temperature were taken at 1m depths weekly using variable resistor thermistors through a hatch in a wharf at the north end of the lake (depth=12-13m), a depth which captures 94% of total lake volume (Oleksy and Richardson 2022). Temperatures were linearly interpolated to daily timescales except if there were more than 14-day gaps in records, which were left as missing data.

Ice phenology trends analysis

All statistical analyses and data visualizations were conducted in R version 4.2.1 (R Core Team, 2022). For the three ice phenology metrics, (ice-off, ice-on, and duration), we calculated Theil-Sen's slopes using formulas from both *zyp* and *trend* packages (Bronaugh & Consortium, 2019; Pohlert, 2020). To test if a

trend was significant, we used the Mann-Kendall rank-based z-score and compared the p-value from that z-score to α=0.05.

To test whether variability of ice is increasing, we used two techniques. First, for visualization, we calculated Bollinger Bands which are one standard deviation above and below a simple moving average and can indicate volatility of a time series (Bollinger, 1992). Second, we calculated the standard deviation of all possible sequential windows of 9-year windows to balance the number of windows with the number of years in each window (Figures S1-S3). We only calculated the standard deviation if > 75% of the 9 years had ice phenology. For each series, we calculated a Theil-Sen's slope and intercept and then used that Theil-Sen's slope and intercept to interpolate across all years. For each year, we calculated the median response along with 5% and 95% quantiles.

Predictors of ice phenology

We used a variety of meteorological metrics as predictors of ice phenology. We calculated the cumulative sum of rain or snow and air temperature data at one-, two-, and three-month intervals for October-December for ice-on predictions and February-April for ice-off predictions. We further calculated fall and spring isotherm dates as the day where a moving average of air temperature crossed a particular temperature threshold (Higgins et al. 2021). We calculated isotherm date for a factorial design using a range of daily air temperature metrics (minimum, mean, maximum), lengths of time (1 to 30 days) and temperature thresholds (0 to 5°C) for 540 unique combinations. We selected the isotherm variable that maximized R^2 for either ice-on or ice-off. The maximum observed air temperature 17 days after 0°C air temperature isotherm was crossed in late winter (hereafter "fall isotherm date") was the strongest linear predictor of ice-on, and the annual date that the daily 29-day mean observed air temperature crossed 4°C (hereafter "spring isotherm date") was the strong linear predictor of ice-off.

We modeled ice-on and ice-off using generalized additive models (GAMs; Hastie & Tibshirani 1990; Wood et al 2016) comprised of terms that accounted for interannual variability across each time series using a gamma family with a logistic link function. We built candidate models based on the top 10

climatic variables that were most highly correlated with either ice-on or ice-off while minimizing collinearity (Figure S4). We fit several GAMs for each ice phenological variable (Table S1) and ultimately selected the models that had the lower AIC and maximized deviance explained (Table S2). We estimated GAMs using the *mgcv* package (version 1.8-40; Wood 2017), visualized all results with the *ggplot2* package (Wickham 2016), and arranged the plots with *patchwork* package (Pedersen 2022).

To examine the effects of broader scale meteorological factors, we built GAMs including global temperature and teleconnections as potential drivers of ice duration. We obtained global annual temperature anomalies averaged over land and ocean from the National Oceanic and Atmospheric Administration (NOAA, 2020). We also considered monthly NAO indices as a predictor of ice phenology, which we downloaded from the National Weather Service Climate Prediction Center (National Weather Service, 2020).

Structural equation modeling for under ice conditions

To examine the effects of ice cover on winter water temperature and spring stratification, we used structural equation modeling (SEM, Grace et al. 2010). We constructed an increasingly complex set of models that linked ice variables (duration, ice-on, and ice-off) with under-water parameters. For all under-ice measurements for each year, we calculated the mean epilimnion temperature (depths 1-3m) and hypolimnion temperature (depths 10-12m). To estimate the magnitude of inverse stratification under-ice, we calculated the difference of water density between 1m and 11m. We also calculated the length of the spring mixed period as the number of days between ice-off and the onset of summer stratification (as in Oleksy and Richardson 2021). To account for varying magnitudes of variables, we mean-centered and unit-variance scaled all variables. We built model relationships to include regressions with causal relationships and covariances between variables that we expected to be colinear rather than causal. We originally built models with ice duration, ice-on, and ice-out but because of a failure to converge, focused on ice duration and ice-out as the two main drivers of water temperature metrics and assigned the ice phenology a covariance structure in the model. To visualize relationships from the optimal SEM, we

calculated partial residual plots by calculating the residuals for the variable using the multiple regression equation from the SEM. We also plotted the component and component plus residual to show where the fitted regression line was located (Wood, 1973). All SEM statistics were calculated using the *lavaan* package (Rosseel 2012) and visualizations were created using the *semPlot* (Epskamp 2022), *ggplotify* (Yu 2021), *ggnetwork* (Briatte 2021), and *cowplot* (Wilke 2020) packages.

Results

Between 1932 and 2022, ice-on dates ranged between December 5th to February 8th with a median of December 27th. Ice-off dates ranged between March 11 and May 2 with a median of April 9th. We observed that ice-on is trending later (slope=0.23 days yr^{-1}, p=0.001, Figure 1) but ice-off is not changing (slope=-0.06 days yr^{-1}. p=0.13, Figure 1). Consequently, ice cover duration is getting shorter (slope=-0.32 days yr^{-1}, p=0.002, Figure 1). Ice-on variance increased by 84% from 8.6 days to 15.9 days, ice-off standard deviation has increased by 48% from 8.2 to 12.2 days, and ice duration variability has increased by 132% from 11.8 to 27.3 days (Figure 2).

Late fall and early winter temperatures were strong controls on the timing of ice-on in Mohonk Lake (Figure 3). The best GAM explained 67.5% of the deviance in the ice-on date with an adjusted R^2 of 0.66 and included a positive linear relationship the timing of the fall isotherm (Figure 3a, Table S2). A smaller proportion of the variance in ice-on day of year could be attributed to cumulative daily mean air temperature in November (Figure 3b). The fall isotherm date has shifted 2.1 days $decade^{-1}$ later since the beginning of the ice monitoring record (p=0.02; Table S3) but there was no trend in cumulative mean daily November air temperature (p>0.05; Figure S5).

Ice-off was controlled by a combination of variables relating to late-winter and spring precipitation and air temperature. The best GAM explained 81.3% of the deviance in the ice-off date with an adjusted R^2 of 0.80 (Table S2). The spring isotherm had a large positive, linear effect on ice-off day (Figure 3c). Cumulative mean daily air temperature in February also had a substantial effect on ice-on date, with warmer years resulting in earlier ice-off (Figure 3d). The amount of snowfall between February

and April had a positive, non-linear impact on ice-off date, such that years with greater amounts of snow were associated with later ice-off, but above a certain snowfall threshold, ice-off date is unaffected (Figure 3e). The spring isotherm shifted earlier by 1.4 days decade^{-1} ($p=0.001$, tau=-3.24), cumulative mean daily air temperature in February increased by 5.9°C decade^{-1} ($p=0.02$, tau=2.21), but cumulative snowfall between February and April did not change substantially (Table S3). Variation in ice duration could be partially explained by trends in global temperature anomaly and variability in November and December NAO cycles (Figure 4, deviance explained 24%).

The selected SEM converged (Figure 5) with a comparative fit index indicating improvement over the null model. All path coefficients were significant ($p<0.05$) except for two relationships with coefficients <0.3. Longer ice durations resulted in higher hypolimnetic (coefficient=0.88, $p=0.001$) and epilimnetic (coefficient=0.66, $p=0.018$) average temperatures under ice (Figure 5c). Warmer hypolimnetic temperatures resulted in more negative water density differences (coefficient=-0.85, $p=0.013$) while warmer epilimnetic temperatures resulted in negligible water density differences (coefficient=1.2, $p<0.001$, Figure 5). Earlier ice-off dates resulted in longer spring mixed periods before summer stratification was established (coefficient=-0.793, $p=0.001$, Figure 5b). Ice duration and ice-off date covaried substantially ($r=0.79$, $p=0.002$). There was not a strong relationship between ice duration on spring mixing length and the covariance of density delta on spring mixing length ($p>0.05$).

Discussion

Mohonk Lake experienced decreases in winter ice-cover that amounted to a loss of approximately one month of winter ice cover over a 90-year period. Trends in ice duration in Mohonk Lake were driven largely by later ice formation and not earlier clearance; although ice-off was not trending earlier, interannual variability in ice-cover increased as in many other seasonally ice-covered lakes (Benson et al., 2012). Overall, decreased ice duration was related to the interplay between global climate change and teleconnections that influenced local weather drivers, in turn driving ice phenology. Specifically, shorter ice duration was associated with higher global temperature anomalies, which were captured in variables

such as increasing fall, winter, and spring air temperatures (Table S3). Additional variation in ice duration was explained by the North Atlantic Oscillation (NAO) in winter (November and December). In years with positive NAO, the northeastern U.S. experiences mild winters while negative NAO are associated with cold-air outbreaks and strong storms, which may promote earlier ice formation or thicker ice cover, respectively. Teleconnections like El Niño and NAO have been similarly shown to modify ice phenology and summer stratification in global lakes (Bai et al., 2012; Sharma & Magnuson, 2014; Oleksy and Richardson 2022), although the effects were location dependent. For example, winter NAO has a substantial effect on spring hypolimnetic temperatures that ultimately carries into the stratified period in deep European lakes (Dokulil et al., 2006).

In Mohonk Lake, ice-on and ice duration changed twice as fast compared to other northern hemisphere lakes (Sharma et al., 2021) and the high rate of change was consistent with other mountain lakes, which show more rapid ice loss than lower-elevation systems (Christianson et al., 2021; Kainz et al., 2017). The rapid change in ice phenology was a result of regional and local climatic shifts. The date when air temperature crossed thresholds that precipitated ice formation (e.g., 0°C) was getting later each late fall and early winter. Consecutive cold days, in combination with cumulative mean daily temperature in November, explained about two-thirds of the variability in ice formation timing on Mohonk Lake, and have resulted in substantially later ice formation over time. Wind is another critical factor in explaining lake ice formation and can modulate lake heat transfer (Read et al., 2012) and may additionally disrupt ice formation when it is still thin (Kirillin et al., 2012), but is missing from our model due to a lack of data availability.

While ice-off in the spring was not changing, preceding seasonal weather patterns explained the majority of interannual variability. Ice-off in Mohonk was controlled by a combination of late winter and early spring air temperatures and cumulative snowfall, consistent with other mountain lakes (Caldwell et al., 2021; Preston et al., 2016; Smits et al., 2020). Warmer conditions in late winter and spring and increases in solar radiation can accelerate ice break-up (Sharma et al., 2013), but this relationship is likely modified by the amount of precipitation that falls on the lake, particularly as snow. In years with more

snowfall, lake ice likely persists longer because it is thicker and the accumulation of snow and associated cold temperatures promote thicker ice formation (Cavaliere et al., 2021).

Changing ice conditions alter under-ice water temperatures in several ways. Since Mohonk is a bedrock-constrained lake in a small watershed with no surface or groundwater inflows, snowmelt likely plays a minimal role in regulating under-ice mixing as in other mountain (Smits et al., 2020) or groundwater intrusion lakes (Kirillin et al., 2012). Instead, under-ice thermal dynamics are likely regulated by a combination of ice duration and ice clarity which determine the degree of radiation-driven convection and mixing (Bruesewitz et al., 2015; Cavaliere et al., 2021). Shorter ice duration was associated with lower hypolimnetic and epilimnetic average water temperatures, and thus resulted in cooler, well-mixed water columns that did not inversely stratify (Woolway et al., 2022). In Mohonk Lake, winters with shorter ice duration, under-ice had weaker inverse stratification and earlier ice-off. This will shorten the phase of stable inverse stratification under the ice (Kirillin et al. 2012; Bruesewitz et al. 2015). The phase before ice-off occurs in the spring can both last weeks or longer with deepening convective layers driven by clear ice and cycles of daily solar radiation (Bruesewitz et al., 2015; Kirillin et al., 2012; Yang et al., 2017).

Together, our results illustrate how the ecological memory of ice phenology manifests in variable summer thermal dynamics (Dugan, 2021; Li et al., 2022). Ice phenology also had a continued effect through to spring conditions with longer spring mixed periods. In years with longer ice seasons, the lake inversely stratified and as the winter transitioned to spring the hypolimnetic water density was closer to maximum density at 4°C. Consequently, the mixed period in the spring was shorter, but the onset of stratification was later (Oleksy & Richardson, 2021). However, when ice clearance occurred earlier, the spring mixing period was longer even with earlier and stronger stratification during the summer (Oleksy & Richardson 2021).

Through changes in thermal dynamics, loss of lake ice has the potential to alter many different biogeochemical and ecological dynamics in lakes. With later ice formation in the fall, more phytoplankton can grow and increase zooplankton overwintering success, dampening the spring

phytoplankton bloom (Hébert et al., 2021). In spring, antecedent winter conditions alter the successional dynamics of phytoplankton assemblages and in turn can result in mismatched phenology of herbivorous zooplankton (Hrycik et al., 2022). With longer mixed seasons and earlier onset of stratification, Mohonk Lake would likely have exacerbated mismatches of zooplankton and phytoplankton spring phenology. Additionally, shorter duration of ice cover and thinner ice promotes higher under-ice metabolism which can account for a substantial amount of annual net ecosystem production (e.g., Brentrup et al., 2021).

While Mohonk Lake is likely not as risk of transitioning from dimictic to monomictic in the next century, the potential for winters with shortening ice phases, intermittent, or no ice cover are within the realm of possibility (Sharma et al., 2019, 2021). Winter limnological studies like this one are critical in "closing the loop" between under-ice and ice-free seasons (Salonen et al., 2009), and underscore repercussions of changing winter ice phenology on lake ecosystem dynamics.

Figures

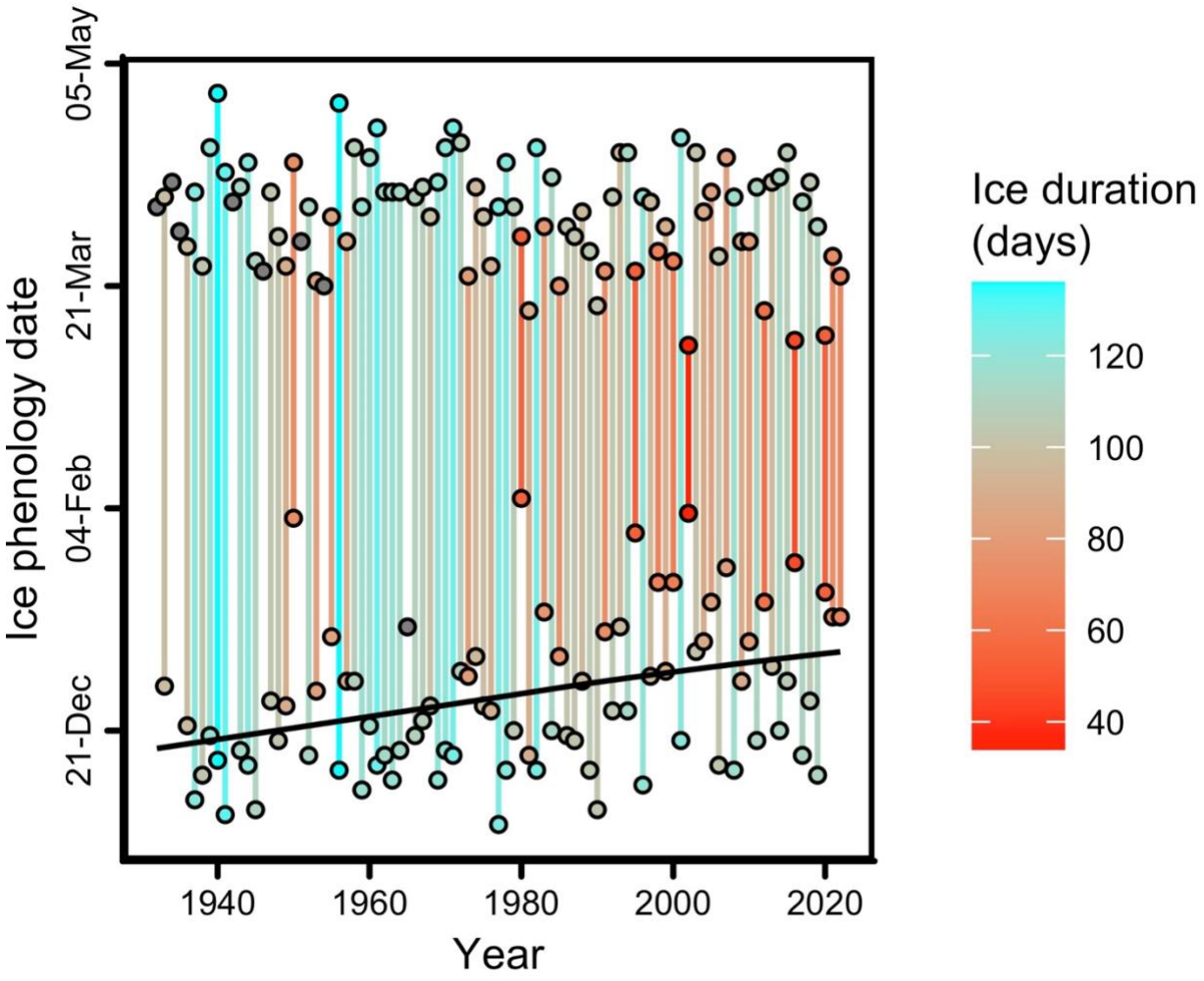

Figure 1. Ice phenology in Mohonk Lake from 1932-2022. Dates of ice-on and ice-off are plotted as points. A line segment connects the ice-on and ice-off in the same water year and the length and color gradient and point fill corresponds to ice-cover duration. Black line indicates significant Theil-Sen's slope ($p<0.05$). Filled grey points indicate years where only ice-on or ice-off was recorded.

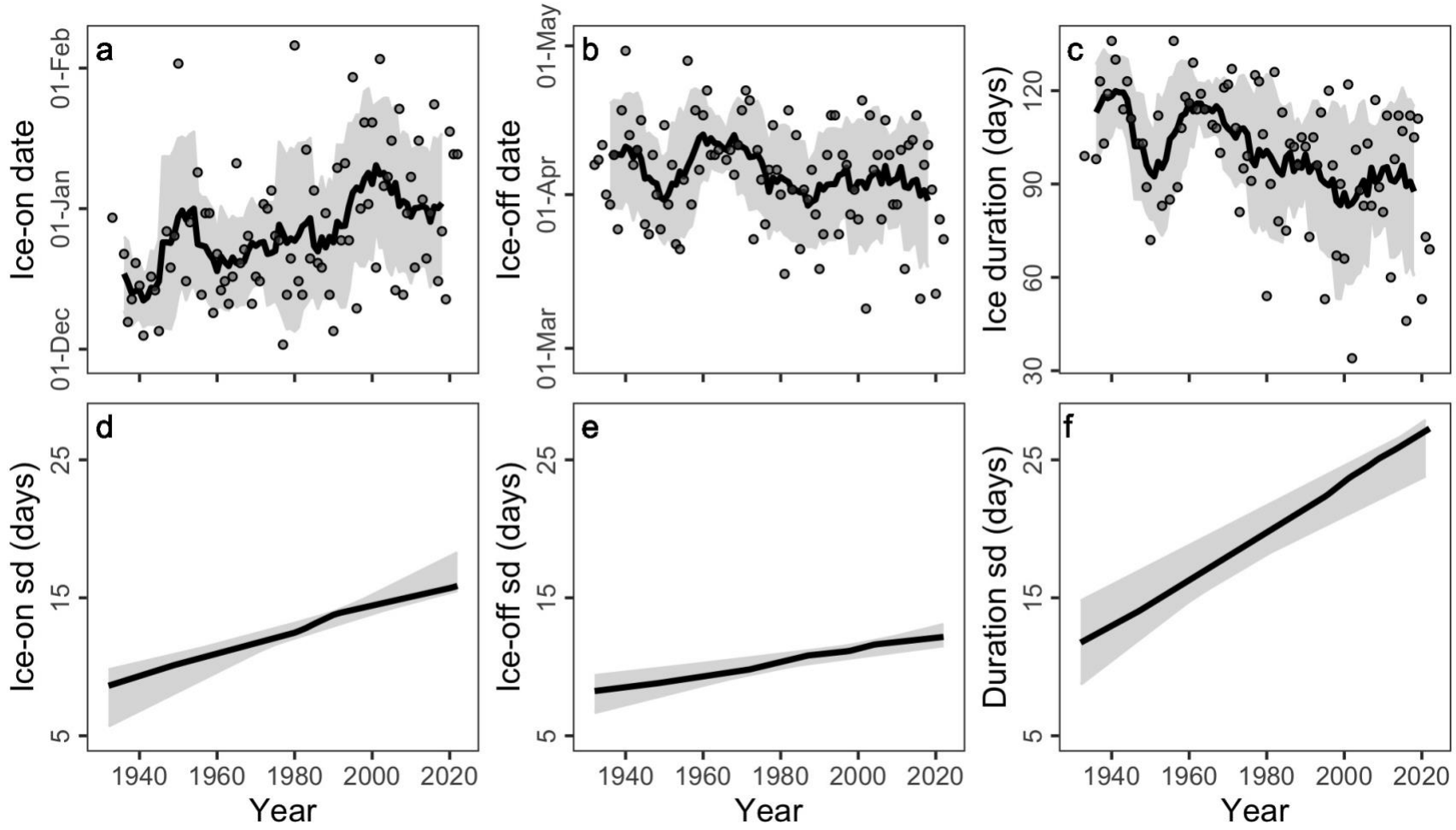

Figure 2. Ice phenology in Mohonk Lake from 1932-2022 for (a) ice-on, (b) ice-off, and (c) ice duration. For each figure, the 9-year simple moving average is presented as the dark line, the Bollinger band (± 9-year rolling standard deviation) is the shaded area presented at the median year for each 9-year window. Standard deviations for all non-overlapping 9-year windows for (d) ice-on, (e) ice-off, and (f) ice duration with shaded areas representing 5% to 95% intervals for each year.

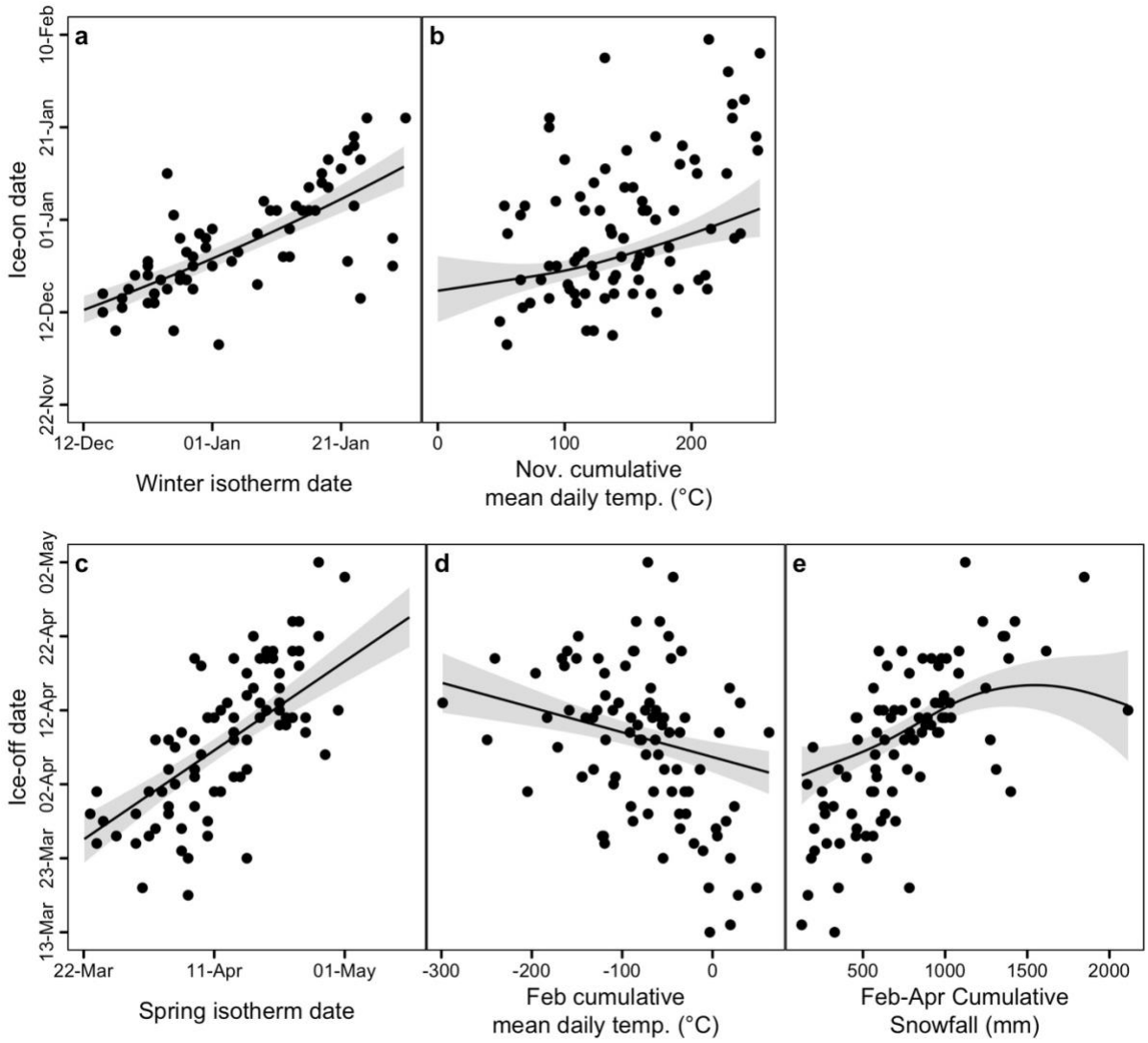

Figure 3. General Additive Model results for ice-on date and ice-off date. Ice-on date was best explained by (a) 17 days after that the maximum daily air temperature fell below the 0°C air temperature isotherm and (b) cumulative mean daily air temperature in November (deviance explained 67.5%). Ice-off date was best explained by (c) 29 days after the average daily air temperature exceeded the 4°C isotherm in the spring, (d) cumulative mean daily temperatures in February, and (e) cumulative snowfall between February and April (deviance explained 81.3%). For all panels, the points represent raw data, and the fitted curves are the predictions holding all other covariates at their median value.

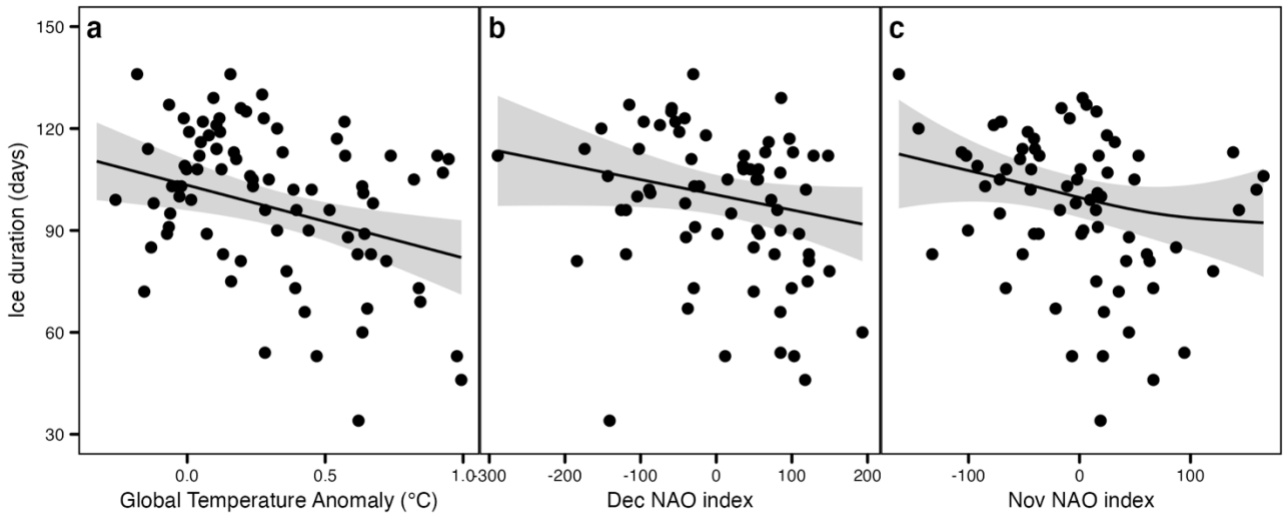

Figure 4. General Additive Model results for global drivers of ice duration. Ice duration was best explained by (a) global temperature anomaly, (b) December NAO index, and (c) November NAO index (deviance explained 24%). For all panels, the points represent raw data, and the fitted curves are the predictions holding all others covariates at their median value.

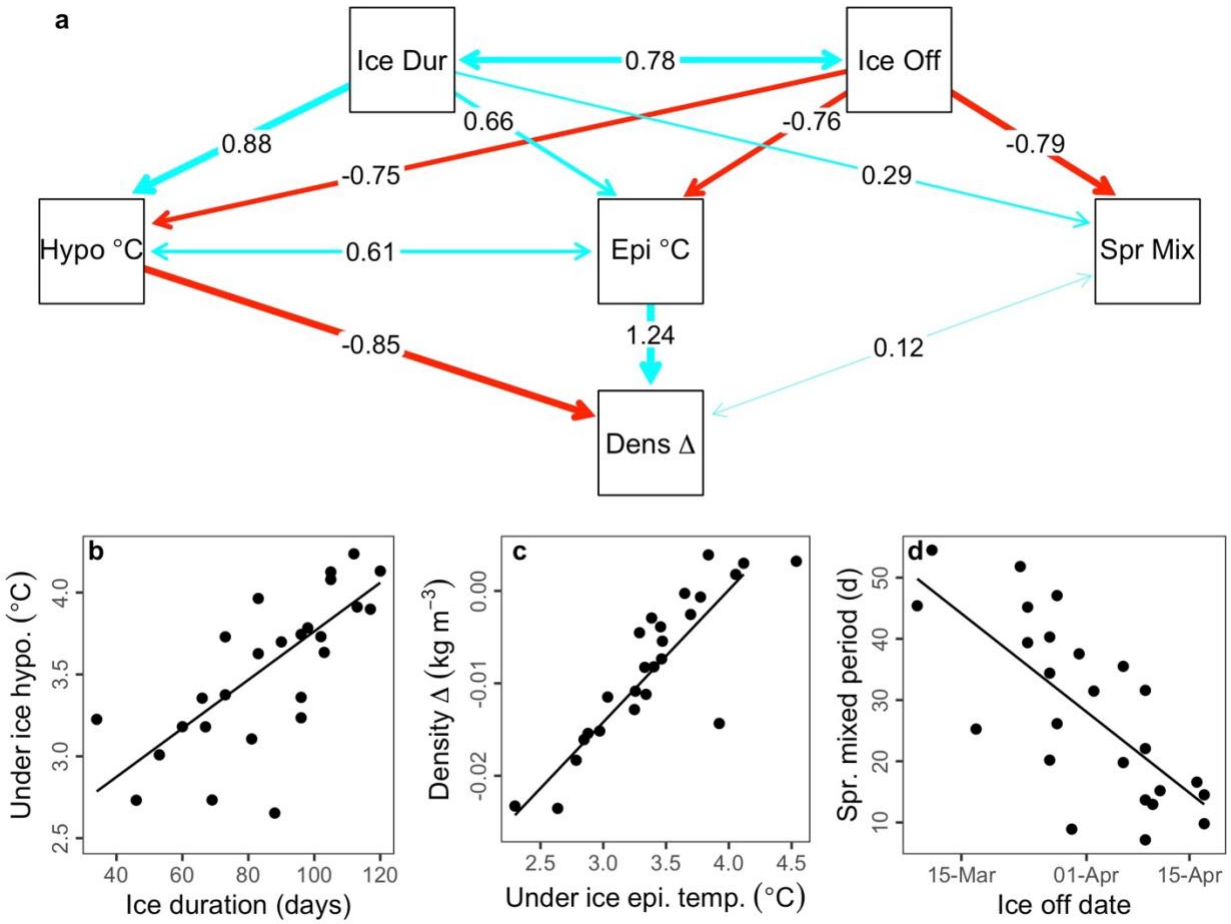

Figure 5. (a) Structural equation model results linking ice duration (Ice Dur) and ice-off (Ice Off) to under ice epilimnetic (Epi °C) and hypolimnetic (Hypo °C) water temperatures, water density difference between 1m and 11m deep (Dens Δ), and the length of the spring mixing period (Spr Mix). Path coefficients in red indicate a negative relationship, green indicates a positive relationship, and the thickness of the edge arrow represents the strength of the relationship between mean-centered and unit-variance scaled variables. Single ended arrows indicate a causal regression while double ended arrows indicate covariance. From the structural equation model, partial residual plots for back-transformed variables are displayed for three relationships including (b) hypolimnetic under ice water temperatures and ice duration, (c) water density difference between 1m and 11m deep and epilimnetic under ice water temperatures, and (d) the length of the spring mixing period and ice-off date.

Acknowledgments

We acknowledge, with respect, that Mohonk Lake is located on the traditional and ancestral homelands of the Munsee Lenape peoples. We thank the original data collectors including Daniel Smiley, Paul Huth, John Thompson, Christy Belardo, Natalie Feldsine, Megan Napoli, Elizabeth Long, and the Mohonk Preserve's Climate Trackers citizen science program. The Mohonk Preserve and Mohonk Mountain House were integral in facilitating long-term monitoring. IAO was supported by National Science Foundation award EPS-2019528. DCR was supported by National Science Foundation DEB-1638575 to Drs. Shannon LaDeau and Kathleen Weathers. We are grateful for Linnea Rock, Carolina Barbosa, and Benjamin Tumolo for helpful feedback on an earlier version of this manuscript.

Author contribution statement:

IAO and DCR co-led the entire manuscript effort, came up with the research questions, designed the study approach, wrote the paper, and contributed equally. IAO conducted the trend and generalized additive model analyses. DCR conducted the structural equation model analyses.

References

Bai, X., Wang, J., Sellinger, C., Clites, A., & Assel, R. (2012). Interannual variability of Great Lakes ice cover and its relationship to NAO and ENSO. *Journal of Geophysical Research: Oceans*, *117*(C3). https://doi.org/10.1029/2010JC006932

Benson, B. J., Magnuson, J. J., Jensen, O. P., Card, V. M., Hodgkins, G., Korhonen, J., Livingstone, D. M., Stewart, K. M., Weyhenmeyer, G. A., & Granin, N. G. (2012). Extreme events, trends, and variability in Northern Hemisphere lake-ice phenology (1855–2005). *Climatic Change*, *112*(2), 299–323. https://doi.org/10.1007/s10584-011-0212-8

Bollinger, J. (1992). Using bollinger bands. *Stocks & Commodities*, *10*(2), 47–51.

Brentrup, J. A., Richardson, D. C., Carey, C. C., Ward, N. K., Bruesewitz, D. A., & Weathers, K. C.

(2021). Under-ice respiration rates shift the annual carbon cycle in the mixed layer of an oligotrophic lake from autotrophy to heterotrophy. *Inland Waters*, *11*(1), 114–123. https://doi.org/10.1080/20442041.2020.1805261

Bruesewitz, D. A., Carey, C. C., Richardson, D. C., & Weathers, K. C. (2015). Under-ice thermal stratification dynamics of a large, deep lake revealed by high-frequency data. *Limnology and Oceanography*, *60*(2), 347–359. https://doi.org/10.1002/lno.10014

Caldwell, T. J., Chandra, S., Albright, T. P., Harpold, A. A., Dilts, T. E., Greenberg, J. A., Sadro, S., & Dettinger, M. D. (2021). Drivers and projections of ice phenology in mountain lakes in the western United States. *Limnology and Oceanography*, *66*(3), 995–1008. https://doi.org/10.1002/lno.11656

Cavaliere, E., Fournier, I. B., Hazuková, V., Rue, G. P., Sadro, S., Berger, S. A., Cotner, J. B., Dugan, H. A., Hampton, S. E., Lottig, N. R., McMeans, B. C., Ozersky, T., Powers, S. M., Rautio, M., & O'Reilly, C. M. (2021). The Lake Ice Continuum Concept: Influence of Winter Conditions on Energy and Ecosystem Dynamics. *Journal of Geophysical Research: Biogeosciences*, *126*(11), 1–20. https://doi.org/10.1029/2020JG006165

Christianson, K. R., Loria, K. A., Blanken, P. D., Caine, N., & Johnson, P. T. J. (2021). On thin ice: Linking elevation and long-term losses of lake ice cover. *Limnology and Oceanography Letters*, *6*(2), 77–84. https://doi.org/10.1002/lol2.10181

Dokulil, M. T., Jagsch, A., George, G. D., Anneville, O., Jankowski, T., Wahl, B., Lenhart, B., Blenckner, T., & Teubner, K. (2006). Twenty years of spatially coherent deepwater warming in lakes across Europe related to the North Atlantic Oscillation. *Limnology and Oceanography*, *51*(6), 2787–2793. https://doi.org/10.4319/lo.2006.51.6.2787

Dugan, H. A. (2021). A Comparison of Ecological Memory of Lake Ice-Off in Eight North-Temperate Lakes. *Journal of Geophysical Research: Biogeosciences*, *126*(6), 1–13. https://doi.org/10.1029/2020jg006232

Hampton, S. E., Galloway, A. W. E., Powers, S. M., Ozersky, T., Woo, K. H., Batt, R. D., Labou, S. G.,

O'Reilly, C. M., Sharma, S., Lottig, N. R., Stanley, E. H., North, R. L., Stockwell, J. D., Adrian, R., Weyhenmeyer, G. A., Arvola, L., Baulch, H. M., Bertani, I., Bowman Jr., L. L., … Xenopoulos, M. A. (2017). Ecology under lake ice. *Ecology Letters*, *20*(1), 98–111. https://doi.org/10.1111/ele.12699

Hébert, M.-P., Beisner, B. E., Rautio, M., & Fussmann, G. F. (2021). Warming winters in lakes: Later ice onset promotes consumer overwintering and shapes springtime planktonic food webs. *Proceedings of the National Academy of Sciences*, *118*(48). https://doi.org/10.1073/PNAS.2114840118

Hrycik, A. R., McFarland, S., Morales-Williams, A., & Stockwell, J. D. (2022). Winter severity shapes spring plankton succession in a small, eutrophic lake. *Hydrobiologia*, *849*(9), 2127–2144. https://doi.org/10.1007/s10750-022-04854-4

Jansen, J., MacIntyre, S., Barrett, D. C., Chin, Y.-P., Cortés, A., Forrest, A. L., Hrycik, A. R., Martin, R., McMeans, B. C., Rautio, M., & Schwefel, R. (2021). Winter Limnology: How do Hydrodynamics and Biogeochemistry Shape Ecosystems Under Ice? *Journal of Geophysical Research: Biogeosciences*, *126*(6), e2020JG006237. https://doi.org/10.1029/2020JG006237

Kainz, M. J., Ptacnik, R., Rasconi, S., & Hager, H. H. (2017). Irregular changes in lake surface water temperature and ice cover in subalpine Lake Lunz, Austria. *Inland Waters*, *7*(1), 27–33. https://doi.org/10.1080/20442041.2017.1294332

Kirillin, G., Leppäranta, M., Terzhevik, A., Granin, N., Bernhardt, J., Engelhardt, C., Efremova, T., Golosov, S., Palshin, N., Sherstyankin, P., Zdorovennova, G., & Zdorovennov, R. (2012). Physics of seasonally ice-covered lakes: A review. *Aquatic Sciences*, *74*(4), 659–682. https://doi.org/10.1007/s00027-012-0279-y

Li, X., Peng, S., Xi, Y., Woolway, R. I., & Liu, G. (2022). Earlier ice loss accelerates lake warming in the Northern Hemisphere. *Nature Communications*, *13*(1), Article 1. https://doi.org/10.1038/s41467-022-32830-y

Magnuson, J. J., Wynne, R. H., Benson, B. J., & Robertson, D. M. (2000). Lake and river ice as a

powerful indicator of past and present climates. *SIL Proceedings, 1922-2010*, *27*(5), 2749–2756. https://doi.org/10.1080/03680770.1998.11898166

Mohonk Preserve, Belardo, C., Feldsine, N., Huth, P., Long, E. C., Napoli, M., Oleksy, I. A., & Richardson, D. C. (2020). *Weekly and high frequency temperature profile data and Secchi depth, Mohonk Lake, NY, USA, 1985 to 2017 ver 1*. Environmental Data Initiative. https://doi.org/10.6073/pasta/7b67399344129afc63cd57e99e778160

Preston, D. L., Caine, N., McKnight, D. M., Williams, M. W., Hell, K., Miller, M. P., Hart, S. J., & Johnson, P. T. J. (2016). Climate regulates alpine lake ice cover phenology and aquatic ecosystem structure. *Geophysical Research Letters*, *43*(10), 5353–5360. https://doi.org/10.1002/2016GL069036

R Core Team. (2022). *R: A Language and Environment for Statistical Computing*. R Foundation for Statistical Computing. https://www.R-project.org/

Read, J. S., Hamilton, D. P., Desai, A. R., Rose, K. C., MacIntyre, S., Lenters, J. D., Smyth, R. L., Hanson, P. C., Cole, J. J., Staehr, P. A., Rusak, J. A., Pierson, D. C., Brookes, J. D., Laas, A., & Wu, C. H. (2012). Lake-size dependency of wind shear and convection as controls on gas exchange: LAKE-SIZE DEPENDENCY OF u_* AND w_*. *Geophysical Research Letters*, *39*(9), n/a-n/a. https://doi.org/10.1029/2012GL051886

Richardson, D. C., Charifson, D. M., Davis, B. A., Farragher, M. J., Krebs, B. S., Long, E. C., Napoli, M., & Wilcove, B. A. (2018). Watershed management and underlying geology in three lakes control divergent responses to decreasing acid precipitation. *Inland Waters*, *8*(1), 70–81. https://doi.org/10.1080/20442041.2018.1428428

Robertson, D. M., Ragotzkie, R. A., & Magnuson, J. J. (1992). Lake ice records used to detect historical and future climatic changes. *Climatic Change*, *21*(4), 407–427. https://doi.org/10.1007/BF00141379

Sharma, S., Blagrave, K., Magnuson, J. J., O'Reilly, C. M., Oliver, S., Batt, R. D., Magee, M. R., Straile, D., Weyhenmeyer, G. A., Winslow, L., & Woolway, R. I. (2019). Widespread loss of lake ice

around the Northern Hemisphere in a warming world. *Nature Climate Change*, *9*(3), Article 3. https://doi.org/10.1038/s41558-018-0393-5

Sharma, S., Filazzola, A., Nguyen, T., Imrit, M. A., Blagrave, K., Bouffard, D., Daly, J., Feldman, H., Feldsine, N., Hendricks-Franssen, H.-J., Granin, N., Hecock, R., L'Abée-Lund, J. H., Hopkins, E., Howk, N., Iacono, M., Knoll, L. B., Korhonen, J., Malmquist, H. J., … Magnuson, J. J. (2022). Long-term ice phenology records spanning up to 578 years for 78 lakes around the Northern Hemisphere. *Scientific Data*, *9*(1), Article 1. https://doi.org/10.1038/s41597-022-01391-6

Sharma, S., & Magnuson, J. J. (2014). Oscillatory dynamics do not mask linear trends in the timing of ice breakup for Northern Hemisphere lakes from 1855 to 2004. *Climatic Change*, *124*(4), 835–847. https://doi.org/10.1007/s10584-014-1125-0

Sharma, S., Magnuson, J. J., Mendoza, G., & Carpenter, S. R. (2013). Influences of local weather, large-scale climatic drivers, and the ca. 11 year solar cycle on lake ice breakup dates; 1905–2004. *Climatic Change*, *118*(3), 857–870. https://doi.org/10.1007/s10584-012-0670-7

Sharma, S., Richardson, D. C., Woolway, R. I., Imrit, M. A., Bouffard, D., Blagrave, K., Daly, J., Filazzola, A., Granin, N., Korhonen, J., Magnuson, J., Marszelewski, W., Matsuzaki, S.-I. S., Perry, W., Robertson, D. M., Rudstam, L. G., Weyhenmeyer, G. A., & Yao, H. (2021). Loss of Ice Cover, Shifting Phenology, and More Extreme Events in Northern Hemisphere Lakes. *Journal of Geophysical Research: Biogeosciences*, *126*(10), e2021JG006348. https://doi.org/10.1029/2021JG006348

Smits, A. P., Macintyre, S., & Sadro, S. (2020). Snowpack determines relative importance of climate factors driving summer lake warming. *Limnology and Oceanography Letters*, *5*(3), Article 3. https://doi.org/10.1002/lol2.10147

Wilkinson, G. M., Walter, J., Fleck, R., & Pace, M. L. (2020). Beyond the trends: The need to understand multiannual dynamics in aquatic ecosystems. *Limnology and Oceanography Letters*, lol2.10153. https://doi.org/10.1002/lol2.10153

Wood, F. S. (1973). The Use of Individual Effects and Residuals in Fitting Equations to Data. *Technometrics*, *15*(4), 677–695. https://doi.org/10.1080/00401706.1973.10489104

Woolway, R. I., Denfeld, B., Tan, Z., Jansen, J., Weyhenmeyer, G. A., & La Fuente, S. (2022). Winter inverse lake stratification under historic and future climate change. *Limnology and Oceanography Letters*, *7*(4), 302–311. https://doi.org/10.1002/lol2.10231

Yang, B., Young, J., Brown, L., & Wells, M. (2017). High-Frequency Observations of Temperature and Dissolved Oxygen Reveal Under-Ice Convection in a Large Lake. *Geophysical Research Letters*, *44*(24), 12,218-12,226. https://doi.org/10.1002/2017GL075373

Supplemental text.

Sequential standard deviation windows: To assess changing variability of ice phenology, we evaluated 3 to 13-year windows of ice-on, ice-off, and ice duration for sequential windows as follows. First, we identified Y different series of standard deviations (Y years where Y=3,...,13) starting with 1932 through 1932+Y-1, beyond which the windows would repeat. Next, for each series, we calculated the standard deviation for sequential windows of Y years. For example, there are four unique versions of the 4-year windows (Fig. S1), nine unique versions of the 9-year windows (Fig. S2), and 13 unique versions of the 13-year windows (Fig. S3). For the 4-year sequential windows, the first version would start in 1932 with standard deviations calculated for 4-year sequential windows: 1932-1936, 1937-1941, etc…, the second version would start in 1933: 1933-1937, 1938-1942, etc… To determine if variability is increasing for each window size, we calculated the Theil-Sens slope and intercept. Ultimately, shorter windows had the most sequential standard deviation windows possible but the least number of unique versions. The 13-year window had only 5 or 6 different sequential standard deviation calculations but the most unique versions. To balance these two factors, we used 9-year windows for both analyses.

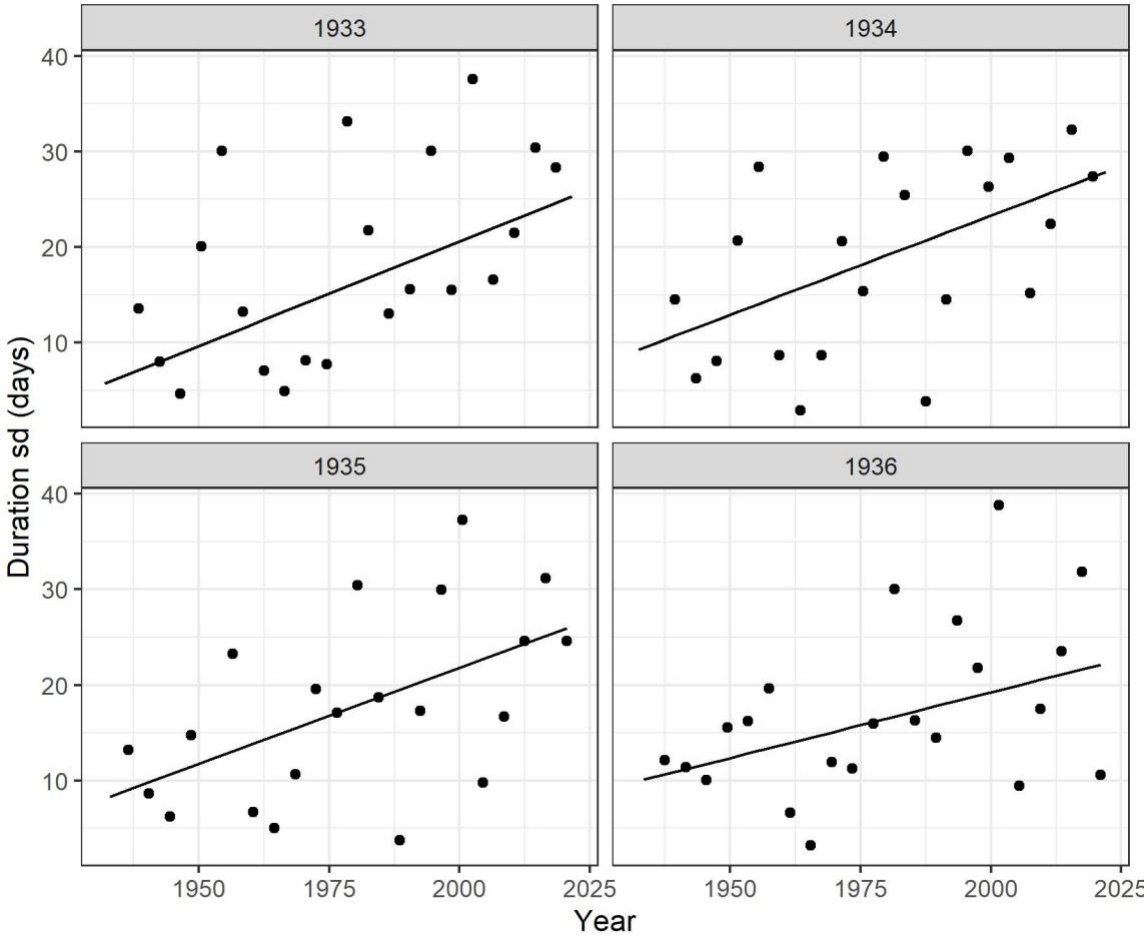

Figure S1. Standard deviations for all possible 4-year sequential windows where the year in each panel's title indicates the start year of the first segment. Additional sequential windows would overlap existing windows. The line indicates the Theil-Sen slope for each sequence of standard deviations.

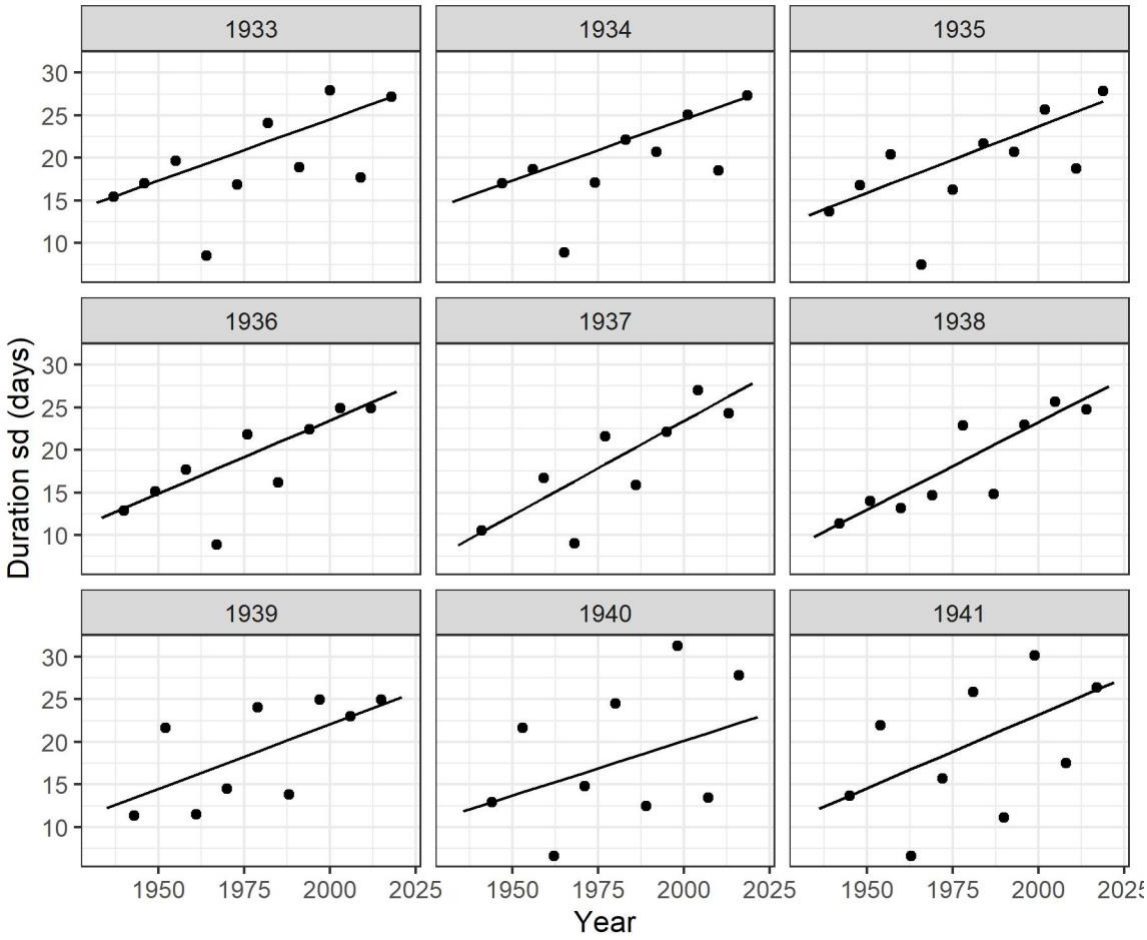

Figure S2. Standard deviations for all possible 9-year sequential windows where the year in each panel's title indicates the start year of the first segment. Additional sequential windows would overlap existing windows. The line indicates the Theil-Sen slope for each sequence of standard deviations.

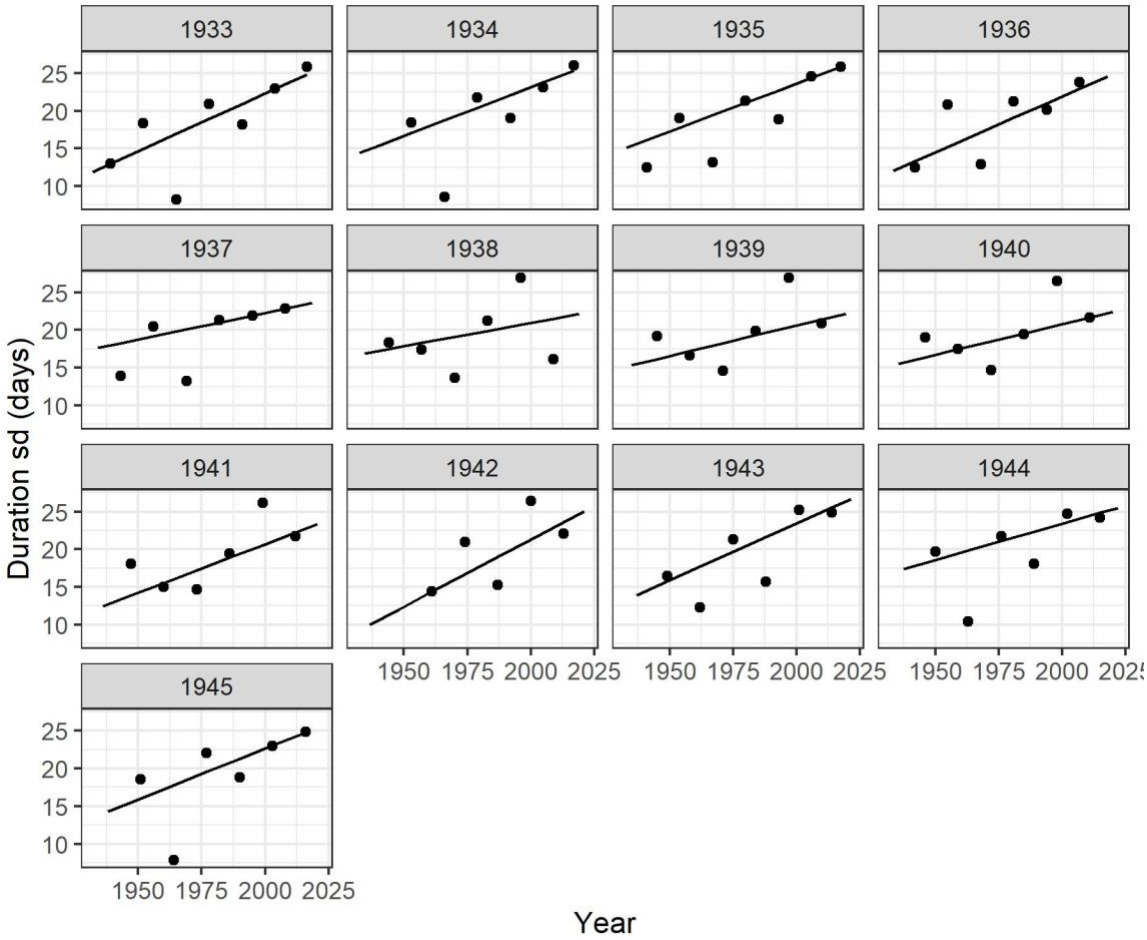

Figure S3. Standard deviations for all possible 13-year sequential windows where the year in each panel's title indicates the start year of the first segment. Additional sequential windows would overlap existing windows. The line indicates the Theil-Sen slope for each sequence of standard deviations.

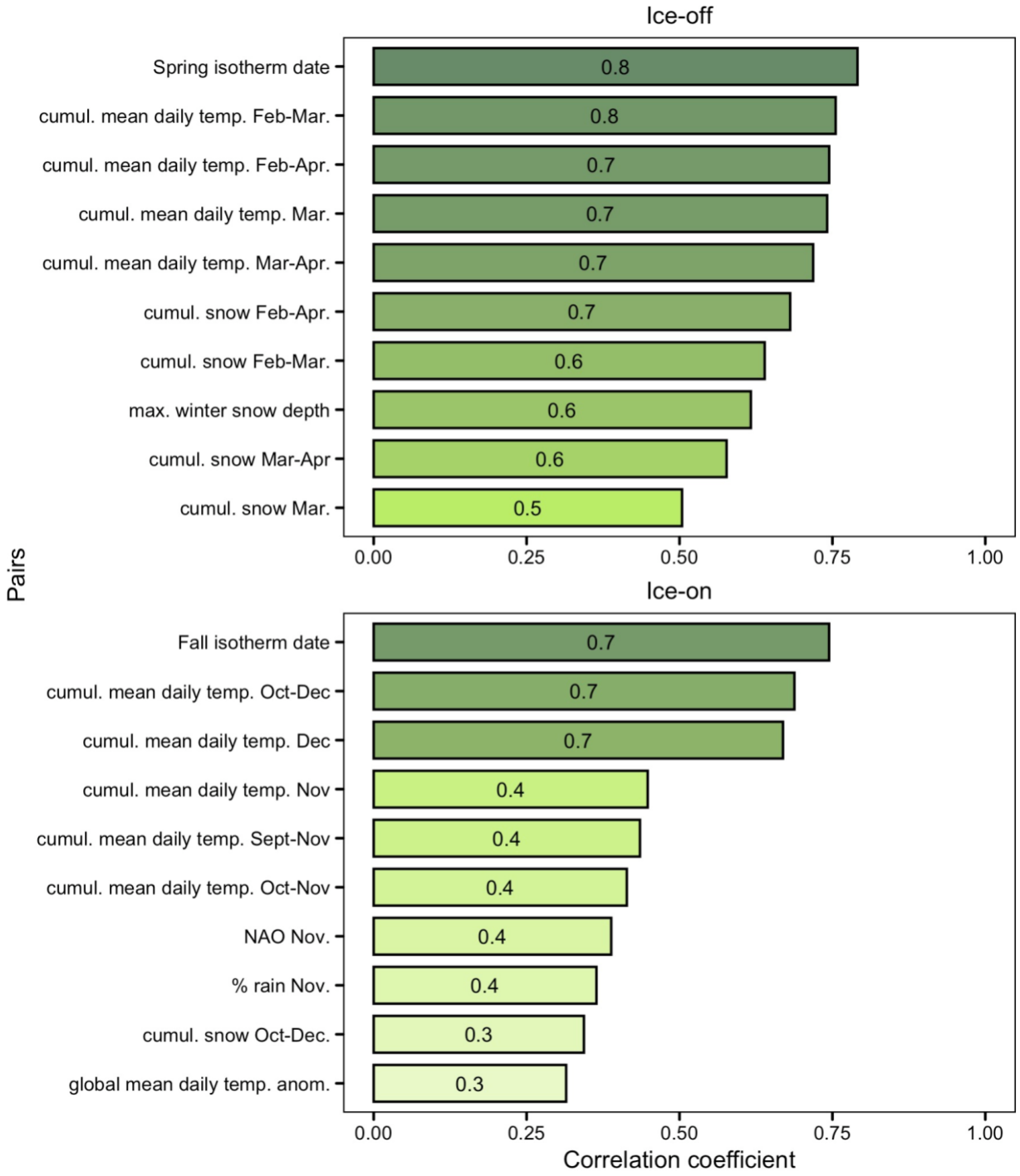

Figure S4. Pairwise correlation (Pearson's r) between ice-off (top panel) and ice-on (bottom panel) and variation meteorological variables ranked in order from strongest to weakest.

Prior to building the models, we tested for collinearity among the variables. For collinear pairs with correlation >|0.7|, we chose the variable with the higher correlation strength with ice-on or ice-off date.

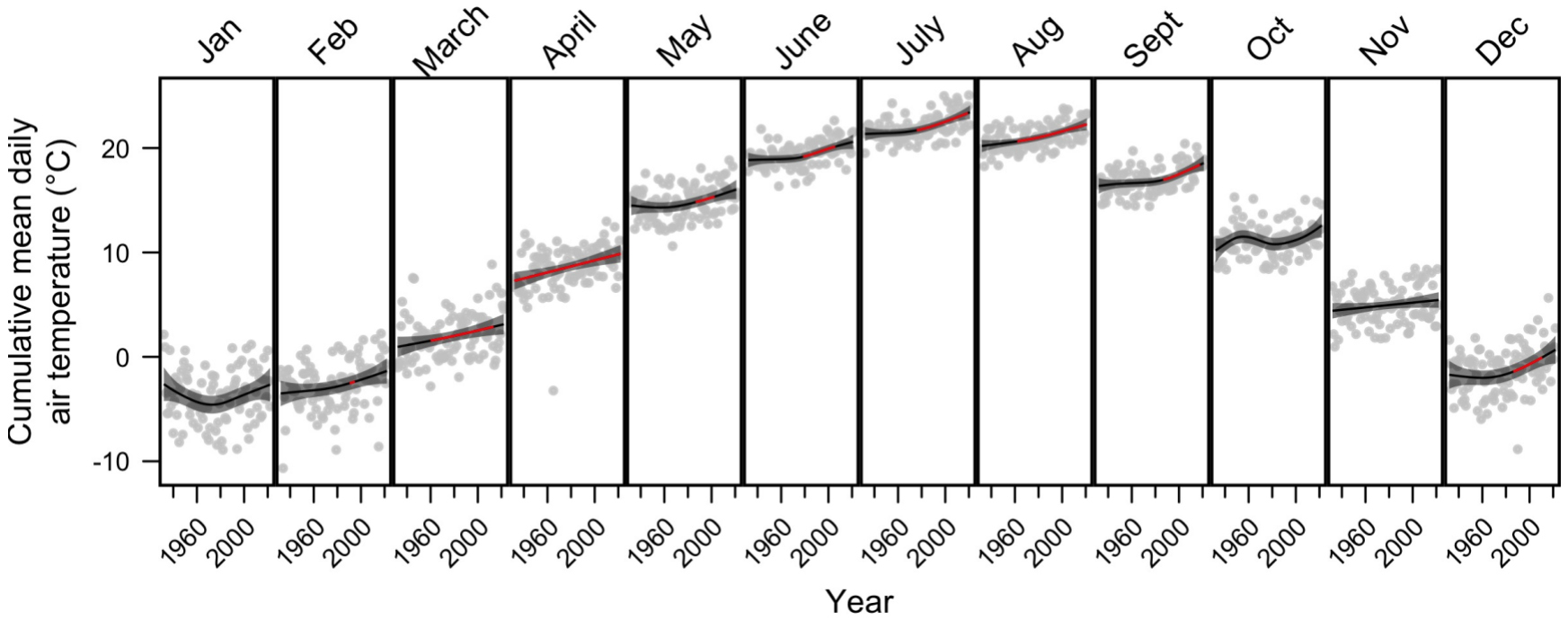

Figure S5. Cumulative mean daily air temperatures at Mohonk Lake between 1932 and 2022. Grey points are raw data and lines are a fitted trend. Shading around trend shows 95% confidence intervals. Red lines indicate periods of a significant temperature increase as indicated by the first derivative of the generalized additive model.

Table S1. List of top 3 GAMs fitted to ice-on and ice-off date. Model complexity (EDF; effective degrees of freedom) and AIC scores are shown for each model. The models highlighted in the text are ranked #1 and model summaries are contained in supplemental Table SX.

Response	Predictors	EDF	AIC	Rank	% Dev. explained
Ice on date	Fall isotherm date, Cumulative mean daily temp. Nov.	3.6	461.8	1	67.7%
Ice on date	Fall isotherm date	2.0	478.9	2	56.4%
Ice on date	Cumulative mean daily air temp. Nov, Cumulative mean daily air temp. Dec	3.0	633.3	3	53.3%
Ice off date	Cumulative mean daily air temp. February, Spring isotherm date, Cumulative snowfall Feb.-Apr., Ice in day of year	6.9	505.3	1	81.8%
Ice off date	Cumulative mean daily air temp. February, Spring isotherm date, Cumulative snowfall Feb.-Apr.	6.5	516.3	2	80.4%
Ice off date	Cumulative mean daily temp. Feb.-Mar., Cumulative snowfall Feb.-Apr., Ice in day of year	8.5	523.7	3	78.2%

Table S2. Top ranking model summary for ice on date and ice off date.

		Estimate	Est. df.	Ref. df	Chi.sq	F	p-value
Ice duration	Intercept	97.6					
	Global temperature anomaly		1.0	1.0	8.2	-	0.0042
	NAO index Nov.		1.4	1.8	4.1	-	0.1387
	NAO index Dec.		1.0	1.0	3.1	-	0.0764
Ice-on date	Intercept	4.4					
	Fall isotherm date		1.0	1.0	-	110.4	< 0.001
	Cumulative mean daily temp. Nov.		1.5	1.9	-	11.8	< 0.001
Ice-off date	Intercept	95.38					
	Cumulative mean daily temp. Feb.		1.0	1.0	-	15.3	< 0.001
	Spring isotherm date		1.0	1.0	-	83.4	< 0.001
	Cumulative snow Feb-Apr.		2.9	3.6	-	8.9	< 0.001
	Ice-on day of year		1.0	1.0	-	1.9	0.16

Table S3. Sens slopes on all the computed climatic variables for Mohonk Lake. We computed Sens slopes for all monthly and seasonal ENSO and NAO variables, but all Sens slope p-values were > 0.05 and therefore not printed in this table.
*** $p < 0.001$; ** $p < 0.01$; * $p < 0.05$.

Climatic variable	**p-value**	**Slope**	**Intercept**	**z-statistic**
Global temp. anomaly (°C)	<0.001***	0.0112	-21.8	9.93
Date of maximum snowfall	0.8183	0.167	-186	0.23
Maximum snow depth (mm)	0.7162	-2.21	4.87e+03	-0.363
Sept. cumulative snow (mm)	1	0	0	0
Sept.-Nov. cumulative rain (mm)	0.114	0.865	-1.4e+03	1.58
Sept.-Nov. number of days mean daily air T below zero	0.0558	-0.0213	46.3	-1.91
Sept.-Nov. number of days min daily air T below zero	0.18	-0.0286	69.9	-1.34
Sept.-Oct. number of days mean daily air T below zero	0.0311*	0	0	-2.16
Sept.-Oct. number of days min daily air T below zero	0.2535	0	1.5	-1.14
Sept. % of precipitation as rain	1	0	100	0
Sept. number of days min daily air T below zero	1	0	0	0
Sept.-Nov. cumulative mean daily air temp. (°C)	0.0011**	1.34	-1.64e+03	3.27
Sept.-Nov. cumulative snow (mm)	0.2629	-0.0577	171	-1.12
Sept.-Oct. cumulative mean daily air temp. (°C)	0.0006***	0.972	-1.06e+03	3.41

Climatic variable	**p-value**	**Slope**	**Intercept**	**z-statistic**
Sept.-Oct. cumulative rain (mm)	0.0203*	0.977	-1.73e+03	2.32
Sept.-Oct. cumulative snow (mm)	0.272	0	0	1.1
Sept. cumulative mean daily air temp. (°C)	0.0001***	0.644	-760	3.9
Sept. cumulative rain (mm)	0.2184	0.371	-631	1.23
Sept. number of days mean daily air T below zero	1	0	0	0
Oct cumulative mean daily air temp. (°C)	0.1013	0.317	-282	1.64
Oct number of days mean daily air T below zero	0.0203*	0	0	-2.32
Oct.-Dec cumulative mean daily air temp. (°C)	0.0033**	1.41	-2.34e+03	2.93
Oct.-Dec. cumulative rain (mm)	0.0287*	0.813	-1.3e+03	2.19
Oct.-Dec. cumulative snow (mm)	0.399	0.798	-1.21e+03	0.843
Oct.-Dec. number of days mean daily air T below zero	0.0025**	-0.0882	198	-3.02
Oct.-Dec. number of days min daily air T below zero	0.0574	-0.0519	143	-1.9
Oct.-Nov cumulative mean daily air temp. (°C)	0.0365*	0.675	-839	2.09
Oct.-Nov. cumulative rain (mm)	0.0435*	0.539	-857	2.02
Oct.-Nov. number of days mean daily air T below zero	0.0511	-0.0204	44.7	-1.95
Oct.-Nov. number of days min daily air T below zero	0.1596	-0.0286	69.8	-1.41

Climatic variable	**p-value**	**Slope**	**Intercept**	**z-statistic**
Oct. % of precipitation as rain	0.282	0	100	-1.08
Oct. cumulative rain (mm)	0.0065**	0.629	-1.15e+03	2.72
Oct. cumulative snow (mm)	0.2791	0	0	1.08
Oct. number of days min daily air T below zero	0.1721	0	1	-1.37
Oct.-Nov. cumulative snow (mm)	0.1781	-0.127	304	-1.35
Nov cumulative mean daily air temp. (°C)	0.2223	0.302	-451	1.22
Nov. % of precipitation as rain	0.0396*	0.0934	-115	2.06
Nov. cumulative rain (mm)	0.4715	-0.136	369	-0.72
Nov. cumulative snow (mm)	0.0551	-0.141	329	-1.92
Nov. number of days mean daily air T below zero	0.0709	-0.0189	41.6	-1.81
Nov. number of days min daily air T below zero	0.3221	-0.0182	48.1	-0.99
Dec. % of precipitation as rain	1	0	26.7	0
Dec. cumulative rain (mm)	0.0735	0.321	-530	1.79
Dec. cumulative snow (mm)	0.2248	1.12	-1.94e+03	1.21
Fall isotherm date	0.02*	0.214	-330	2.25
Dec. number of days mean daily air T below zero	0.0181*	-0.0588	134	-2.36

Climatic variable	p-value	Slope	Intercept	z-statistic
Dec. number of days min daily air T below zero	0.176	-0.0196	64.2	-1.35
Dec. cumulative mean daily air temp. (°C)	0.0046**	0.78	-1.58e+03	2.84
Jan cumulative rain (mm)	0.9045	0.0201	41.5	0.12
Jan-Mar cumulative mean daily air temp. (°C)	0.0183*	1.39	-2.9e+03	2.36
Jan-Mar. cumulative rain (mm)	0.3423	0.326	-378	0.95
Jan-Mar. cumulative snow (mm)	0.8747	-0.207	1.41e+03	-0.158
Jan. % of precipitation as rain	0.959	0.0015	18.1	0.0514
Jan. cumulative mean daily air temp. (°C)	0.624	0.198	-513	0.49
Jan. cumulative snow (mm)	0.9317	0	343	-0.0857
Jan. number of days mean daily air T below zero	0.6182	0	24	-0.498
Jan. number of days min daily air T below zero	0.1583	0	29	-1.41
Feb cumulative mean daily air temp. (°C)	0.0268*	0.599	-1.26e+03	2.21
Feb-Apr. cumulative mean daily air temp. (°C)	0.0001***	2.34	-4.39e+03	4.03
Feb-Apr. cumulative rain (mm)	0.6143	0.155	-36.7	0.504
Feb-Apr. cumulative snow (mm)	0.6858	-0.714	2.12e+03	-0.405
Feb-Mar cumulative mean daily air temp. (°C)	0.0021**	1.43	-2.85e+03	3.07

Climatic variable	p-value	Slope	Intercept	z-statistic
Feb-Mar. cumulative rain (mm)	0.6264	0.121	-62.6	0.487
Feb-Mar. cumulative snow (mm)	0.8855	-0.186	1.01e+03	-0.144
Feb-Mar. number of days mean daily air T above zero	0.0011**	0.0968	-162	3.27
Feb-Mar. number of days min daily air T above zero	0.0003***	0.087	-161	3.63
Feb. % of precipitation as rain	0.6708	0.016	-13.7	0.425
Feb. cumulative rain (mm)	0.5928	0.0635	-49.8	0.535
Feb. cumulative snow (mm)	0.6808	-0.341	1.01e+03	-0.411
Feb. number of days mean daily air T below zero	0.0496*	-0.037	92.7	-1.96
Feb. number of days min daily air T below zero	0.0036**	-0.0263	77.8	-2.91
Mar-Apr cumulative mean daily air temp. (°C)	0.0002***	1.59	-2.82e+03	3.79
Mar-Apr. cumulative rain (mm)	0.7865	0.0889	16.5	0.271
Mar-Apr. cumulative snow (mm)	0.2235	-0.998	2.3e+03	-1.22
Mar-Apr. number of days mean daily air T above zero	0.0029**	0.0625	-73.9	2.98
Mar-Apr. number of days min daily air T above zero	0.0007***	0.0923	-150	3.4
Mar. % of precipitation as rain	0.3528	0.0534	-79.9	0.929
Spring isotherm date	0.001***	-0.143	474	-3.24

Climatic variable	p-value	Slope	Intercept	z-statistic
Mar. cumulative mean daily air temp. (°C)	0.0042**	0.833	-1.59e+03	2.86
Mar. cumulative rain (mm)	0.5833	0.0939	-91.4	0.548
Mar. cumulative snow (mm)	0.5213	-0.468	1.2e+03	-0.641
Mar. number of days mean daily air T above zero	0.0032**	0.0615	-102	2.95
Mar. number of days mean daily air T below zero	0.0032**	-0.0615	133	-2.95
Mar. number of days min daily air T above zero	0.0062**	0.0545	-99.4	2.73
Mar. number of days min daily air T below zero	0.0062**	-0.0545	130	-2.73
Apr. % of precipitation as rain	0.1598	0	92.9	1.41
Apr. cumulative mean daily air temp. (°C)	0.0002***	0.84	-1.4e+03	3.69
Apr. cumulative rain (mm)	0.7112	-0.0739	249	-0.37
Apr. cumulative snow (mm)	0.1652	0	7.62	-1.39
Apr. number of days mean daily air T below zero	0.1745	0	0	-1.36
Apr. number of days min daily air T below zero	0.0034**	-0.04	85.1	-2.93